Effect of thermal fatigue on the mechanical properties of a continuous composite fiber used for car clutch facings

Camille Flament, Bruno Berthel, Michelle Salvia, Gérard Crosland, Isabelle Alix

Effect of thermal fatigue on the mechanical properties of a continuous composite fiber used for car clutch facings

Camille Flament[1,2], Bruno Berthel[1,a], Michelle Salvia[1,b], Gérard Crosland[2], Isabelle Alix[1]

[1] Ecole Centrale de Lyon, LTDS UMR5513, 69134 Ecully Cedex, France,
[2]VALEO Matériaux de Friction, 87000 Limoges, France

Abstract. In dry clutch systems, the clutch facing is an annular shaped continuous fibre composite, with an organic matrix, which transmits the torque from the engine to the wheels. In use it is submitted to thermo-mechanical cycling. Due to the composite fibre organisation, the strain field under thermo-mechanical loading is not homogenous. Full field data is needed to describe the material behaviour. Digital Image Stereo-Correlation was used to determine the coefficients of thermal expansion of the material. To determine the effect of temperature and cyclic loading on the mechanical properties, the composite was subjected to different thermal cycles. The material properties are modified with increasing temperature and number of cycles. These results were confirmed by dynamic mechanical analysis which showed thermal ageing of the resin. The local information given by the strain fields revealed a non-uniform evolution of the material properties with thermal cycling. Moreover, optical investigation and tensile tests also show an evolution of the damage of the material with the thermal cycles.

1 Introduction

During dry clutch engagement, sliding contact occurs between the clutch facing and the counterfaces: flywheel and pressure plate (cast iron materials). When sliding occurs, heat is generated according to the dissipation mechanisms of kinetic energy. Temperature increase can be high in case of repetitive engagement (up to 250°C or 300°C, depending on clutch technology). This study focuses on the effect of thermal cycling on the mechanical properties of car clutch facings. The thermo-mechanical behavior of fiber-reinforced composites depends on matrix composition, fiber properties and fiber orientation. The manufacturing process of the studied composite makes it is difficult to define an elementary representative volume. An experimental set up was therefore designed to conduct tests on the whole specimen. Digital Image Stereo Correlation (DISC) is one of the most popular full-field measurement techniques. It is an optic contactless experimental technique, measuring full-field displacement and strain with sub-pixel accuracy. This technique is used to assess the mechanical and thermal properties of a wide range of materials [1–7], and is therefore an interesting means of analyzing local thermal behavior. The clutch facing alone was non-planar, as it was not kept flat by the clutch system. Therefore, it was necessary to resort to a stereo vision system, which makes it possible to study non-planar specimens and out-of-plane displacement.

[a] Corresponding author: bruno.berthel@ec-lyon.fr
[b] Corresponding author: michelle.salvia@ec-lyon.fr

The objectives of this paper are threefold: firstly, to present a new experimental method to measure thermal expansion of a composite part using the digital image stereo correlation technique; secondly, to apply this method on a continuous fiber-reinforced friction material used in vehicles and to assess the effects of thermal cycling on the coefficients of thermal expansion; and lastly, to analyze results through complementary techniques. The first part of the paper describes the clutch facing and, in particular, the fiber organization. Then the experimental set up and experimental procedure are presented, followed by results. The results are then analysed through complementary techniques.

2 Clutch facing material

The material studied was the organic clutch facing that transmits the rotary motion from the engine to the wheels. It is an annular shaped continuous fiber composite comprising a fiberglass yarn fitted with copper strips. The composite matrix is mainly composed of phenolic thermosetting resin. The steps of the process are described in [8]. The yarn is impregnated with the resin and dried, then is shaped into a preform before being put into a heated mould and pressed and cured. The end-product has grooves and rivet holes. However, to have better understanding of the structure, the study was conducted on ungrooved and unbored specimens. The structure had external and internal diameters of 240 and 160 mm respectively, and was 2.5 mm thick. During the preforming operation, a machine guides the impregnated fibers, coupling uniform rotation to radial translation. The two movements have different frequencies, resulting in a fiber organization presented in Figure 1. The actual fiber organization of the clutch facing is, in general, very heterogeneous, as some movements during preforming and curing can modify the impregnated yarn tracing.

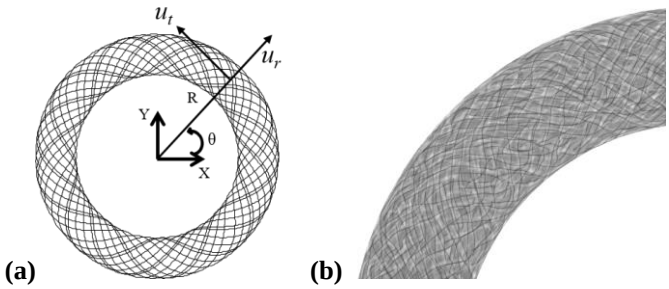

Figure 1: (a) Schematic preform and (b) X Ray tomographic view of a clutch facing.

3 Experimental set-up and post-processing

3.1 coefficients of thermal expansion

The coefficient of thermal expansion describes material behavior under thermal loading. It is defined, in the simplest form, as the fractional increase in length per unit rise temperature (coefficient of linear thermal expansion). In the case of small deformation, the fractional increase in length is equivalent to the strain tensor (ε), and the CTE tensor can be expressed as follows:

$$\underline{\underline{\varepsilon}} = \underline{\underline{CTE}}\ \Delta T \tag{1}$$

where $\underline{\underline{\varepsilon}}$ is the strain tensor, ΔT the temperature variation and $\underline{\underline{CTE}}$ the coefficient of thermal expansion tensor.

The CTE is defined in its linear form over a limited temperature range. For certain materials and larger temperature ranges, it depends on temperature. In the present study, the temperature range was

30°C to 300°C. Previous investigations confirmed the orthotropic behavior of the annular clutch facing. In this case, the coefficients of thermal expansion are finally determined using equation below:

$$\begin{bmatrix} CTE_R & 0 & 0 \\ 0 & CTE_T & 0 \\ 0 & 0 & CTE_z \end{bmatrix} = \frac{1}{\Delta T} \begin{bmatrix} \varepsilon_R & 0 & 0 \\ 0 & \varepsilon_T & 0 \\ 0 & 0 & \varepsilon_z \end{bmatrix} \quad (2)$$

where ε_R, ε_T and ε_z (respectively CTE_R, CTE_T and CTE_z) are the tangential, radial and *z* components of the strain (respectively coefficient of thermal expansion), see Figure 1(a).

In this study, only the radial and tangential components of the CTE tensor were calculated. In order to analyze the effects of thermal cycling on the coefficients of thermal expansion, the following variable has been defined:

$$D_i = \frac{CTE_i(N) - CTE_i(0)}{CTE_i(0)} \quad (3)$$

where $i=R$ or T and N is the number of thermal cycles.

3.2 Experimental set-up

Considering the orthotropic axes of the material, strains were determined in the cylindrical coordinate system. In this study, strain fields were measured with the Digital Image Stereo-Correlation (DISC) technique. The Digital Image Correlation (DIC) technique provides displacement and strain fields on the surface of deformed specimens. Digital Image Stereo-Correlation (DISC or 3D-DIC) is based on pairs of simultaneous images and combines temporal and stereoscopic matching. The DISC method makes the difference between in plane strain and out of plane displacements and gives access to 3D profiles of in plane strain fields. The system used in our laboratory is Vic 3D developed by Correlated Solutions [9]. Thermal testing was carried out in a climate chamber developed by France Etuves. To have optical access to the specimen, the chamber was equipped with a window on the top. The image capturing system consisted of two CCD cameras (AVT Pike F-421B) with 2,048 x 2,048 pixels resolution. The cameras' field of view was 250x250 mm. Therefore 1 pixel on the CCD sensor corresponded to a 0.12 mm square on the specimen. Two thermocouples were fixed onto the rear side of the specimen and inside the climate chamber respectively. The device is shown in Figure 2. During the calibration procedure, the calibration target was placed inside the chamber so that the cameras viewed it through the window. During calibration, distortion in the optical path was calculated and taken into account in the algorithm [10].

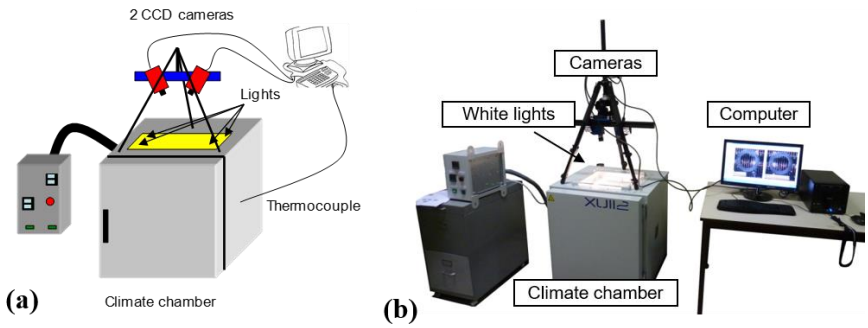

Figure 2: (a) Outline and (b) photo of the experimental set up.

3.3 Experimental procedure and post-processing

The specimen was painted with black and white spray paint to create a speckle pattern with adequate contrast. Then, it was placed inside the climate chamber, with no restraints, in a horizontal position. To measure strain due to free thermal expansion, pairs of images were taken at room temperature, defining the reference state of the object. Then the temperature was increased progressively. Images were taken every 25°C from 50°C to 300°C, at which point specimen temperature was stabilized. In order to reduce the impact of noise, twelve pair of images were taken in a stabilized and averaged images were used to calculate strain fields. The strain resolution varied from 0.01% to 0.05% strain depending on temperature. In the end, equation (2) was used to determine the coefficients of thermal expansion. The experimental device was validated with known materials (pure aluminum, aluminum oxide and uni-directional carbon-fiber-reinforced bismaleimide) before being applied to the clutch facing. To study the effects of thermal cycling on the coefficients of thermal expansion of the composite, the following thermal cycles were repeated (Figure 3). The coefficients of thermal expansion were then measured after 6, 25, 50, 75 and 100 cycles.

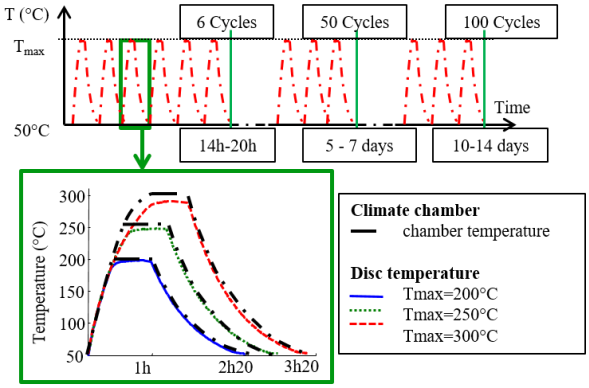

Figure 3: Thermal cycles

4 Results

To determine the global effect of thermal cycling, the evolution of the average CTE with the number of thermal cycles was measured for the three maximum temperatures (Figure 4(a) and (b)). Three clutch facings were tested per condition. As the number of cycles increases, the material expands less than the as-received material. The evolution also depends on the maximum cycle temperature: the drop of CTE_R is around 50% for the 300°C cycles and under 6% for the 200°C cycles. The experimental set up gives access to strain fields and therefore to local information on the evolution of the CTE. Analysing the strain maps in details revealed inhomogeneous evolution of the CTE with thermal cycling (Figure 4(c)). Some areas see an increase of the CTE whereas others see a decrease. This could be the sign of competing degradation mechanisms during thermal cycles. Comparing global and local effect revealed that, even though the 200°C cycles did not seem to affect the clutch facing, the modified zone represents 30% of the surface of the annular disc.

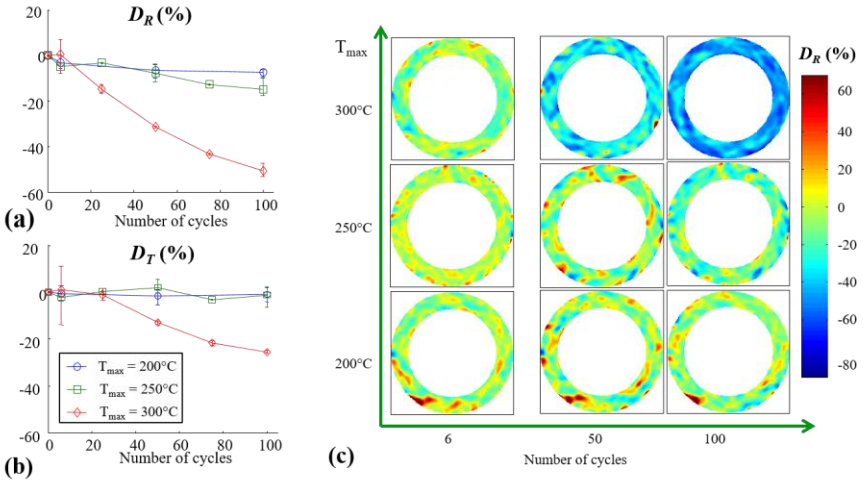

Figure 4: (a) and (b) : global evolution of D_R and D_T ; (c) local evolution of D_R for each maximal temperature after 6, 50 and 100 cycles.

5 Discussions

Measures of the thermal expansion for different maximum temperatures revealed a non-homogeneous evolution of the material behaviour. To understand the root causes of these effects complementary analysis were done.

First, crack process was investigated. To begin with, surfaces of specimens were observed employing optical microscopy. The number and length of cracks were measured on 12x12 mm² surface. The evolution with the number of thermal cycles is presented Figure 5(b). No cracks were found for the specimen that was cycled at 200°C. Cumulated crack length for the 300°C cycled specimen reach 50 mm after 100 cycles, twice as much as the 250°C cycled specimen. The cracks mainly ran along the fibre bundle / matrix interface (Figure 5(a)). The difference in thermal expansion of the glass fibre (around $5*10^{-6}$ /K) and the phenolic resin (around $15*10^{-6}$ /K) causes thermal stress in the composite which can cause damage if the loading is cyclic. Resin degradation can also explain the presence of cracks. Furthermore acoustic emission (AE) signals were used to detect volume damage on tensile specimens that were thermally cycled at 200°C and 300°C [11]. After six cycles, the specimens were tested under monotonic tensile load with AE sensors detecting AE signals. These measures revealed volume damage of the 200°C cycled specimens that was neither visible on the stress–strain curve nor on the surface of the specimen (Figure 5(c)).

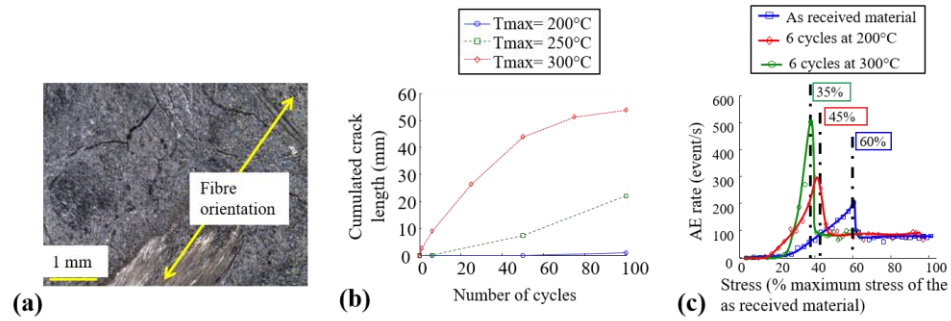

Figure 5: (a) A 2mm crack after 100 cycles at 250°C; (b) cumulated crack length ; (c)Acoustic emission rate versus stress for the as received and thermally cycled material.

Secondly, Dynamic Mechanical Analysis (DMA) was made. DMA is the observation of time-dependant behaviour of material under dynamic periodic sinusoidal strain or stress. The DMA tests were conducted on a 50N 0.1dB Metravib test machine. Specimens were cut into the disc (size 40x12x2.5 mm). This test is destructive. The evolution of the storage modulus (*E*') and loss factor (tan δ) were measured during a tension/compression dynamic test (1Hz, +/-5 µm displacement, -100°C up to 400°C at 1°C/min). Under thermo-mechanical loading, the behaviour of the as-received material is characterised by a relaxation phenomena of a component of the resin around 40°C. The storage modulus (*E*') drops around this temperature. Thermal degradation occurs over 280°C (Figure 6).

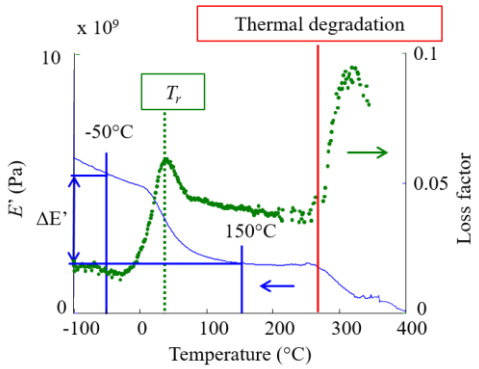

Figure 6: Storage modulus and loss factor of the as-received material

The relaxation temperature (T_r) and *E*' under and above T_r were measured (*cf.* Figure 6). The storage modulus difference between under and above T_r is named Δ*E*'. When cycled at 200°C, the specimen relaxation temperature and storage modulus above T_r are almost not affected by thermal cycling. For cycling temperature over 200°C, T_r increases with the number of cycles and seems to reach a plateau (Figure 7(a)). The rise may be caused by additional cross linking formation with thermal ageing. This is confirmed by a decrease of Δ*E*' with thermal cycling (Figure 7(c)). In fact, studies have shown that around 250°C, condensation reactions could happen in phenol-form resins creating additional cross links [12,13]. However, *E*' under T_r decreases when the specimens are cycled at 250°C or 300°C (Figure 7(b)). This could be the consequence of the presence of cracks due to thermal cycling.

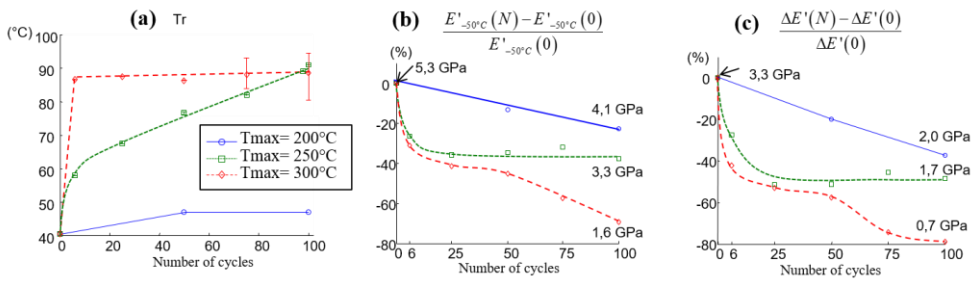

Figure 7: Evolution of T_r (a), storage modulus *E*' (for T=-50°C) (c) and Δ*E*'(b).

6 Conclusion

The evolution of certain thermo-mechanical properties with thermal cycling and maximum cycle temperature were studied. The clutch facing is almost not affected by 100 cycles at 200°C. For higher temperature, thermal ageing and damage was found. On the one hand, the presence of cracks in the

matrix can be observed by optical investigation. Crack are caused by differential expansion and resin degradation over 280°C and the consequence is for example the decrease of the stiffness of the material as it is seen Figure 7(b). Furthermore, measures of damage using AE done on a specimen under monotonic tensile tests confirm that thermal cycling cause volume damage. On the other hand, resin transformation and probably additional cross linking due to thermal ageing of the matrix can be observed around 250°C. The modification of the resin and the cracks nucleation must contribute to the decrease of the CET. The interaction of these complex thermal degradation mechanisms lead to a non-homogenous evolution of the CTE (Figure 4).

To finish, it is important to stress the fact that the imposed thermal cycling is very severe due to the homogeneous heating of the part. In reality, the clutch facing is submitted to a high but very short increase of the temperature and only on the sliding surface.

References

1 P. Bing, X. Hui-min, H. Tao, A. Asundi, Polym. Test. **28** (2009)
2 U. Eitner, M. Köntges, R. Brendel, Sol. Energy Mater. Sol. Cells. **94** (2010)
3 O. De Almeida, F. Lagattu, J. Brillaud, Compos. Part A Appl. Sci. Manuf. **39** (2008)
4 M. Grédiac, Compos. Part A Appl. Sci. Manuf. **35** (2004)
5 L. Robert, F. Nazaret, T. Cutard, J.-J. Orteu, Exp. Mech. **47** (2007)
6 S.V. Lomov, P. Boisse, E. Deluycker, F. Morestin, K. Vanclooster, D. Vandepitte, I. Verpoest, a. Willems, Compos. Part A Appl. Sci. Manuf. **39** (2008)
7 T.-I. Lee, M.S. Kim, T.-S. Kim, Polym. Test. **51** (2016)
8 M. Bezzazi, A. Khamlichi, Mater. Des. **28** (2007)
9 Correlated Solutions.Inc, (n.d.).
10 J.-J. Orteu, Opt. Lasers Eng. **47** (2009)
11 C. Flament, M. Salvia, B. Berthel, G. Crosland, J. Compos. Mater. **50** (2015)
12 M. Křístková, P. Filip, Z. Weiss, R. Peter, Polym. Degrad. Stab. **84** (2004)
13 Y. Chen, Z. Chen, S. Xiao, H. Liu, Thermochim. Acta. **476** (2008)